ChemComm

Cite this: *Chem. Commun.*, 2012, **48**, 8329–8331

www.rsc.org/chemcomm

COMMUNICATION

Photocatalytic production of hydrogen peroxide by two-electron reduction of dioxygen with carbon-neutral oxalate using a 2-phenyl-4-(1-naphthyl)quinolinium ion as a robust photocatalyst†

Yusuke Yamada,[a] Akifumi Nomura,[a] Takamitsu Miyahigashi[a] and Shunichi Fukuzumi*[ab]

Received 11th June 2012, Accepted 26th June 2012
DOI: 10.1039/c2cc34170k

Efficient photocatalytic production of hydrogen peroxide (H_2O_2) from O_2 and oxalate has been made possible by using a 2-phenyl-4-(1-naphthyl)quinolinium ion as a robust photocatalyst in an oxygen-saturated mixed solution of a buffer and acetonitrile with a high quantum yield of 14% (maximum 50% for the two-electron process) at λ = 334 nm and a high H_2O_2 yield of 93% at λ > 340 nm.

Hydrogen peroxide (H_2O_2) has been recognized not only as a clean oxidant but also as a selective oxidant for various oxidation processes.[1] H_2O_2 is also a potential candidate for a clean liquid fuel in the next generation, because H_2O_2 generates electric power by using an H_2O_2 fuel cell and emits only water and oxygen after the reaction.[2] Currently H_2O_2 supplied to industry is mainly produced by the anthraquinone process, which requires costly hydrogen and large energy consumption for extraction of H_2O_2 from an organic reaction medium.[3] A much simpler and less energy consuming process should be developed for the wide applications of H_2O_2.

H_2O_2 can be simply prepared by reduction of atmospheric O_2 by an organic molecule, which possesses high reducing ability. Oxalate is a compound capable of acting as a strong reductant (E^0 = −0.475 V *vs.* NHE)[4a] and can be easily found in soil and leaves of various vegetables in a high content of ~1 wt%.[4b] Thus, a natural system utilizes oxalate as an electron donor for producing H_2O_2 in the enzymatic active centre of oxalate oxidase, which catalyzes the oxidation of oxalate, reduction of O_2 to H_2O_2 and formation of two moles of CO_2 [eqn (1)].[5]

$$(COOH)_2 + O_2 \rightarrow 2CO_2 + H_2O_2 \qquad (1)$$

In this process, CO_2 is solely produced as a by-product. A property of oxalate, which can be converted into CO_2 after oxidation, benefits efficient photocatalytic reactions because of prevention of back electron transfer. Photocatalytic H_2O_2 production *via* the O_2 reduction using various electron donors such as alcohols and acetic acid has been examined by various systems using semiconductors[6] or organic photosensitizers.[7] It is desired to use oxalate as an electron donor for the photocatalytic production of H_2O_2, because oxalate stored in the edible plants is easily extracted with boiling water but disposed as a waste material. However, such carbon-neutral oxalate has yet to be utilized as an efficient electron donor in previous reports,[8] because oxalate includes the C–C bond which is kinetically stable under ambient conditions.[9]

Herein, we report photocatalytic H_2O_2 production by O_2 reduction with oxalate as an electron donor using a 2-phenyl-4-(1-naphthyl)quinolinium ion ($QuPh^+$–NA, Scheme 1a), which forms the long-lived electron-transfer state upon the photoexcitation with strong oxidation ability, as a photocatalyst.[10] In the photocatalytic system, the quantum yield of H_2O_2 production was determined by a conventional method using an actinometer. Nanosecond laser flash photolysis and kinetic measurements were performed to reveal that the quinolinyl radical ($QuPh^{\bullet}$–$NA^{\bullet+}$) produced by the photoirradiation of $QuPh^+$–NA reduces O_2 to produce H_2O_2 as indicated in Scheme 1b.

The photocatalytic H_2O_2 production has been performed by photoirradiation (λ > 340 nm) of an oxygen-saturated (1.3 mM) mixed solution (2.0 mL) of a phosphate buffer (300 mM, pH 6.0; pH was adjusted by NaOH) and acetonitrile (MeCN) [1 : 1 (v/v)] containing $QuPh^+$–NA (0.22 mM) and oxalate (1.5 mM). Fig. 1 shows the time courses of H_2O_2 and CO_2 production in the photocatalytic reaction. From the slopes of these lines in Fig. 1, the rate of CO_2 evolution was determined to be 0.45 μmol h^{-1}, which is nearly double of H_2O_2 production rate of 0.23 μmol h^{-1}, in agreement with the stoichiometry in eqn (1).

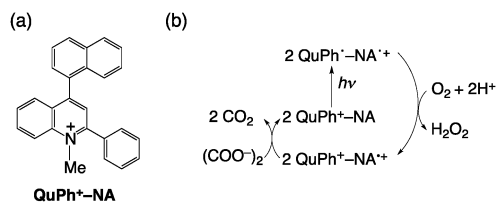

Scheme 1 (a) Structure of $QuPh^+$–NA and (b) the overall photocatalytic cycles for H_2O_2 production.

[a] *Department of Material and Life Science, Division of Advanced Science and Biotechnology, Graduate School of Engineering, Osaka University, ALCA, Japan Science and Technology Agency (JST), Suita, Osaka 565-0871, Japan. E-mail: fukuzumi@chem.eng.osaka-u.ac.jp*
[b] *Department of Bioinspired Science, Ewha Womans University, Seoul 120-750, Korea*

† Electronic supplementary information (ESI) available: Experimental procedures, time courses of H_2O_2 production (Fig. S1), CV of oxalic acid (Fig. S2), quantum yield determination (Fig. S3) and transient absorption spectra in the presence of O_2 (Fig. S4). See DOI: 10.1039/c2cc34170k

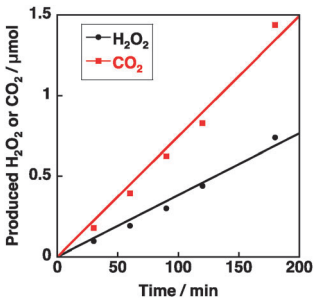

Fig. 1 Time courses of H_2O_2 and CO_2 production. The photocatalytic production of H_2O_2 and CO_2 was performed by photoirradiation (λ > 340 nm) of an oxygen-saturated mixed solution (2.0 mL) of a phosphate buffer (pH 6.0) and MeCN [1 : 1 (v/v)] containing $QuPh^+$–NA (0.22 mM) and oxalate (1.5 mM).

The photocatalytic H_2O_2 production was executed using oxalate with different concentrations ranging from 1.5 mM to 6.0 mM and $QuPh^+$–NA (0.22 mM) in a mixed solution of a phosphate buffer (200 mM, pH 7.0) and MeCN [1 : 1 (v/v), 2.0 mL] as shown in Fig. S1 in ESI.† The concentration of H_2O_2 in the reaction solution increased linearly for initial 200 min and then the H_2O_2 production rate decreased at prolonged irradiation time due to the consumption of oxalate. The initial (90 min) H_2O_2 production rates increased from 0.53 μmol h^{-1} (1.5 mM oxalate) to 1.6 μmol h^{-1} (6.0 mM oxalate) in proportion to the concentration of oxalate. The H_2O_2 yields calculated based on oxalate reached 93% in the solution containing 1.5 mM oxalate. The maximum concentration of oxalate in the mixed solution is 6.0 mM, however, a further increase in oxalate concentration is possible in a mixed solution of pure water and MeCN [1 : 1 (v/v)]. Upon increasing the concentration of oxalate to 12 mM, the initial (30 min) reaction rate reached 6.3 μmol h^{-1}. On the other hand, the H_2O_2 yield was less than 30%, because of an increase in pH during the reaction. A further increase in the concentration of oxalate to 200 mM did not lead to a dramatic increase in the H_2O_2 production rate.

The efficiency of the photocatalytic reaction can be evaluated by the quantum yield (Φ) of the products, where the Φ value was defined as the mole number of H_2O_2 produced divided by that of photons absorbed by the photocatalyst. In previous reports, the Φ value of H_2O_2 production has been determined to be 4.2% by photoirradiation (340 nm) of an oxygen-saturated buffer (pH 7.5–8.0) containing ZnO colloid and oxalate.[8a] The Φ value of the H_2O_2 production in a mixed solution of water and MeCN [1 : 1 (v/v)] containing $QuPh^+$–NA (0.057 mM) and oxalate (200 mM) was determined using a ferrioxalate actinometer to be 14% (Fig. S3, ESI†), which is more than three times of the Φ value obtained with ZnO. Such high quantum yield is originated from the high oxidizing and reducing ability of photogenarated $QuPh^{\bullet}$–$NA^{\bullet+}$, E_{red} = 1.87 V and E_{ox} = −0.90 V *vs.* SCE in MeCN, which are sufficient for oxidation of oxalate and reduction of O_2.[10]

The robustness of the photocatalytic system for H_2O_2 production was also examined by photoirradiation (λ > 340 nm) of an oxygen-saturated mixed solution (2.0 mL) of a buffer (pH 7.0) and MeCN containing $QuPh^+$–NA (0.22 mM) and oxalate (3.0 mM). The calculated amount of oxalic acid was added to a reaction solution after each reaction for four times. The relative activity of each reaction cycle is indicated in Fig. 2a in terms of H_2O_2 production rates referring to the first cycle. More than 90% activity of the first cycle was maintained for each cycle with the H_2O_2 yield of each cycle higher than 75%. Oxalate acts as a two-electron reductant, thus, the total turnover number of $QuPh^+$–NA for five cycles reached more than 100. The robustness of $QuPh^+$–NA was also assured by insignificant change in the UV-vis spectra. Fig. 2b compares the UV-vis absorption of the solutions before starting the photocatalytic reaction (solid line) and after the 5th cycle (dashed line). Thus, the organic photocatalyst of $QuPh^+$–NA is stable during the recycling tests.

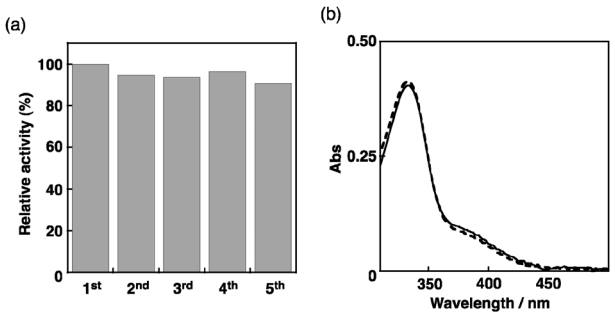

Fig. 2 (a) Recyclability tests of H_2O_2 production under photoirradiation (λ > 340 nm) of an oxygen-saturated mixed solution (2.0 mL) of a buffer solution (pH 7.0) and MeCN [1 : 1 (v/v)] containing $QuPh^+$–NA (0.22 mM) and $(COOH)_2$ (3.0 mM). Relative activity of each cycle was determined by referring to the catalytic activity of the 1st cycle. (b) UV-vis absorption spectra of the solutions before starting the photocatalytic reaction (solid line) and after the 5th cycle (dashed line).

Laser flash photolysis measurements of $QuPh^+$–NA were conducted to detect the electron-transfer state ($QuPh^{\bullet}$–$NA^{\bullet+}$) in the absence and presence of oxalate as shown in Fig. 3. Laser excitation at 355 nm of a mixed solution of an aqueous buffer (pH 7.0) and MeCN [1 : 1 (v/v)] containing $QuPh^+$–NA (0.056 mM) results in formation of the electron-transfer state ($QuPh^{\bullet}$–$NA^{\bullet+}$) with a quantum yield of 0.34, which is well matched with the previously reported value.[10,11] Formation of $QuPh^{\bullet}$–$NA^{\bullet+}$ was confirmed by the transient absorption at λ_{max} = 420 nm ($QuPh^{\bullet}$ moiety) and 690 nm ($NA^{\bullet+}$ moiety) at 2.4 μs after photoirradiation of the solution in the absence of oxalate as shown in Fig. 3a.[10,11] Additionally, a broad band appearing at around 1000 nm evidences formation of the π-dimer radical cation, [($QuPh^{\bullet}$–$NA^{\bullet+}$)-($QuPh^+$–NA)], in the solution.[10,11] In the presence of oxalate (6.0 mM), the decay behaviour of these characteristic bands in Fig. 3b differs from the case in the absence of oxalate in Fig. 3a.

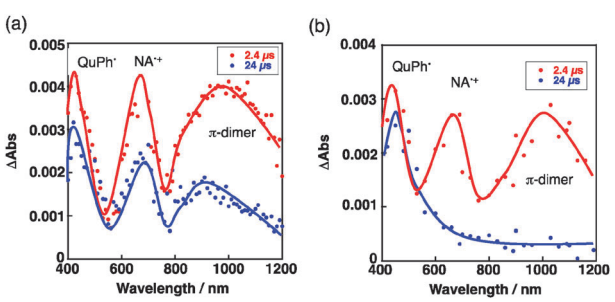

Fig. 3 Transient absorption spectra of $QuPh^+$–NA (0.056 mM) in a mixed solution of a deaerated phosphate buffer (pH 7.0) and MeCN [1 : 1 (v/v)] at 298 K taken at 2.4 μs (red) and 24 μs (blue) after nanosecond laser excitation at 355 nm (a) in the absence and (b) in the presence of oxalic acid (6.0 mM).

The absorption band at λ = 420 nm remained at 24 μs after photoexcitation, on the other hand, the absorption bands at λ = 690 nm and at around 1000 nm assigned to the $NA^{\bullet+}$ and π-dimer radical cation, respectively,[10,11] disappeared in this period. This observation suggests that electron transfer from oxalate to the $NA^{\bullet+}$ moiety of the π-dimer radical cation occurs as predicted by the higher one-electron reduction potential of the $NA^{\bullet+}$ moiety (E_{red} = 1.87 V *vs.* SCE)[10] than the onset oxidation potential of oxalate (0.80 V *vs.* SCE in a deaerated mixed solution of a buffer and MeCN [1 : 1 (v/v)] as shown in Fig. S2 in ESI†).

The electron transfer from oxalate to the $NA^{\bullet+}$ moiety of the π-dimer radical cation was monitored by the decay curves of absorption at 690 nm at various concentrations of oxalate as shown in Fig. 4a. The rate obeyed pseudo-first-order kinetics and the pseudo-first-order rate constant (k_{obs}) increased linearly with increasing concentration of oxalate. The second-order rate constant (k_{ox}) of electron transfer from oxalate to the $NA^{\bullet+}$ moiety of the π-dimer radical cation was determined from the slope of a linear plot in Fig. 4b to be 1.6×10^7 M^{-1} s^{-1}.

The electron transfer from $QuPh^{\bullet}$ to oxygen was monitored by the decay curves of absorption at 420 nm shown in Fig. 4c in the presence of various concentrations of oxygen. The rate obeyed pseudo-first-order kinetics and the pseudo-first-order rate constant (k_{obs}) increased in proportion to concentration of oxygen. The second-order rate constant ($k_{red(O_2)}$) of electron transfer from $QuPh^{\bullet}$ to O_2 was determined from the slope of a linear plot in Fig. 4d to be 4.6×10^9 M^{-1} s^{-1}, which is close to the diffusion limited value.[12] The second-order rate constant of electron transfer from oxalate to the $NA^{\bullet+}$ moiety was 1.6×10^7 M^{-1} s^{-1}, which is only 1/300 of $k_{red(O_2)}$. Thus, in the reaction solution, the reduction of O_2 by $QuPh^{\bullet}$–$NA^{+\bullet}$ is faster than the oxidation of oxalate even though the concentration of O_2 (1.3 mM) is smaller than the concentration of oxalate (0–6 mM). These values support the reaction mechanism shown in Scheme 1b, in which the O_2 reduction by $QuPh^{\bullet}$ occurs first and then the remaining electron transfer from $(COO^-)_2$ to $NA^{\bullet+}$ occurs to oxidize oxalate.

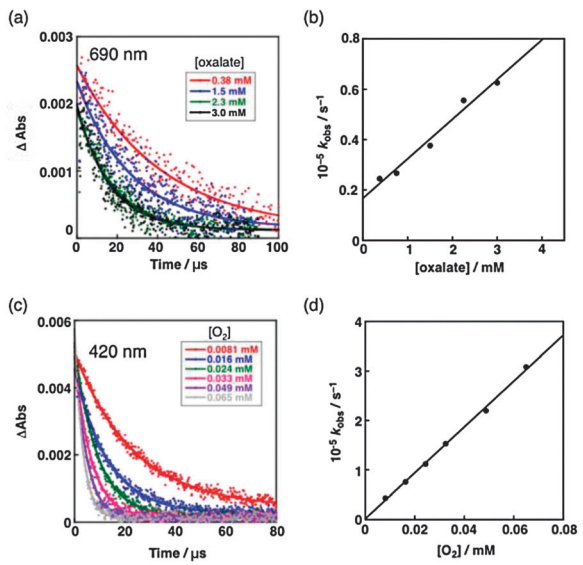

Fig. 4 (a) Decay time profile of absorption at 690 nm due to $QuPh^{\bullet}$–$NA^{\bullet+}$ at various concentrations of oxalate (0.38 mM, red; 1.50 mM, blue; 2.3 mM, green; 3.0 mM, black) in the presence of $QuPh^{+}$–NA (0.056 mM). $QuPh^{\bullet}$–$NA^{\bullet+}$ was produced by the laser excitation (λ = 355 nm) of a deaerated mixed solution of a phosphate buffer (pH 7.0) and MeCN [1 : 1 (v/v)]. (b) Plot of the pseudo-first-order rate constant (k_{obs}) for electron transfer from oxalate to $QuPh^{\bullet}$–$NA^{\bullet+}$ *vs.* [oxalate]. (c) Decay time profile of absorption at 420 nm due to $QuPh^{\bullet}$–$NA^{\bullet+}$ with various concentrations of O_2 (red, 0.0081 mM; blue, 0.016 mM; green, 0.024 mM; pink, 0.033 mM; purple, 0.049 and gray, 0.065 mM) in the presence of $QuPh^{+}$–NA (0.056 mM). (d) Plot of the pseudo-first-order rate constant (k_{obs}) for electron transfer from $QuPh^{\bullet}$–$NA^{\bullet+}$ to O_2 *vs.* [O_2].

This is the first report to produce H_2O_2 with oxalate using an electron donor–acceptor linked dyad as a robust photocatalyst. Oxalate acts as an efficient electron donor in the photocatalytic two-electron reduction of O_2 to produce H_2O_2 with a high Φ value (14%). Laser flash photolysis measurements manifested that electron transfer from the photogenerated π-dimer radical cation [($QuPh^{\bullet}$–$NA^{\bullet+}$)($QuPh^{+}$–NA)] to O_2 occurs first to afford $QuPh^{+}$–$NA^{\bullet+}$, followed by electron transfer from oxalate to $NA^{\bullet+}$.

This work was supported by Grants-in-Aid (No. 20108010 to S.F. and 24350069 to Y.Y.) from the Ministry of Education, Culture, Sports, Science and Technology, Japan and NRF/MEST of Korea through the WCU (R31-2008-000-10010-0) and GRL (2010-00353) Programs.

Notes and references

1 (*a*) M. K. Tse, S. Bhor, M. Klawonn, G. Anilkumar, H. Jiao, A. Spannenberg, C. Döbler, W. Mägerlein, H. Hugl and M. Beller, *Chem.–Eur. J.*, 2006, **16**, 1875; (*b*) *Catalytic Oxidations with Hydrogen Peroxide as Oxidant*, ed. G. Strukul, Kluwer Academic, Dordrecht, The Netherlands, 1992.
2 (*a*) Y. Yamada, S. Yoshida, T. Honda and S. Fukuzumi, *Energy Environ. Sci.*, 2011, **4**, 2822; (*b*) A. E. Sanli and A. Aytac, *Int. J. Hydrogen Energy*, 2011, **36**, 869; (*c*) S. Fukuzumi, Y. Yamada and K. D. Karlin, *Electrochim. Acta*, 2012, DOI: 10.1016/j.electacta.2012.03.132, in press.
3 (*a*) E. Santacesaria, M. D. Serio, R. Veloti and U. Leone, *Ind. Eng. Chem. Res.*, 1994, **33**, 277; (*b*) D. Hancu and E. J. Beckman, *Ind. Eng. Chem. Res.*, 1999, **38**, 2833; (*c*) D. Hancu and E. J. Beckman, *Ind. Eng. Chem. Res.*, 2000, **39**, 2843.
4 (*a*) *Standard Potentials in Aqueous Solution*, ed. A. J. Bard, R. Parsons and J. Jordan, Marcel Dekker, New York, 1985; (*b*) D. B. Haytowitz and R. H. Matthews, *Agriculture Handbook No. 8–11*, Science and Education Administration, USDA, Washington, D.C., 1984.
5 A. Hodgkinson, *Oxalic Acid in Biology and Medicine*, Academic Press, London, 1977.
6 (*a*) M. Teranishi, S. Naya and H. Tada, *J. Am. Chem. Soc.*, 2010, **132**, 7850; (*b*) D. Tsukamoto, A. Shiro, Y. Shiraishi, Y. Sugano, S. Ichikawa, S. Tanaka and T. Hirai, *ACS Catal.*, 2012, **2**, 599; (*c*) V. Maurino, C. Minero, G. Mariella and E. Pelizzetti, *Chem. Commun.*, 2005, 2627.
7 (*a*) M. Fukushima, K. Tatsumi, S. Tanaka and H. Nakamura, *Environ. Sci. Technol.*, 1998, **32**, 3948; (*b*) S. Fukuzumi, S. Kuroda and T. Tanaka, *J. Am. Chem. Soc.*, 1985, **107**, 3020.
8 (*a*) A. J. Hoffman, E. R. Carraway and M. R. Hoffmann, *Environ. Sci. Technol.*, 1994, **28**, 776; (*b*) T. R. Rubin, J. G. Calvert, G. T. Rankin and W. MacNevin, *J. Phys. Chem.*, 1953, **75**, 2850.
9 S. Yamazaki, Y. Yamada, N. Fujiwara, T. Ioroi, Z. Shiroma, H. Senoh and K. Yasuda, *J. Electroanal. Chem.*, 2007, **602**, 96.
10 H. Kotani, K. Ohkubo and S. Fukuzumi, *Faraday Discuss.*, 2012, **155**, 89.
11 Y. Yamada, T. Miyahigashi, H. Kotani, K. Ohkubo and S. Fukuzumi, *J. Am. Chem. Soc.*, 2011, **133**, 16136.
12 (*a*) S. Fukuzumi, H. Miyao, K. Ohkubo and T. Suenobu, *J. Phys. Chem. A*, 2005, **109**, 3285; (*b*) S. Fukuzumi and S. Kuroda, *Res. Chem. Intermed.*, 1999, **25**, 789.